INTER-PULSE CODING FOR IDEAL RANGE RESPONSE

Nadav Levanon

Department of Electrical Engineering - Systems, Tel Aviv University
Chaim Levanon Street, 69978, Tel Aviv, Israel
phone: + (972) 3 6408137, fax: + (972) 3 6407095, email: nadav@eng.tau.ac.il
web: www.eng.tau.ac.il/~nadav/index.html

Keywords: Radar, Pulse compression, High PRF, Ipatov coding.

ABSTRACT

A different way to increase the energy within a coherent processing interval (CPI) is suggested – many short dense pulses with inter-pulse coding instead of few widely-spaced long pulses with intra-pulse coding. Long coded pulses result in masking targets at close range and suffer from poor Doppler tolerance. We overcome the range ambiguity, inherent to dense pulses (high PRF), by inter-pulse coding. Ideal range response (no ambiguity, no sidelobes) can be obtained, e.g., by using a binary periodic Ipatov sequence for inter-pulse coding. The periodic property is maintained as long as the number of transmitted periods exceeds the number of processed periods by at least two.

1. INTRODUCTION

The probability of detection in coherent radar depends on the signal energy contained in the coherent processing interval (CPI). The Doppler (velocity) resolution depends on the duration of the CPI; hence the use of a coherent train of pulses. The delay (range) resolution depends on the bandwidth of the signal, which prompts using narrow pulses or modulated long pulses.

Increasing the energy in a CPI of a given duration, without increasing the peak power and without degrading the delay resolution, can be accomplished by using longer pulses or more pulses. A good review of the tradeoffs was given by Long and Harriger [1].

Two of the problems associated with long modulated pulses are: (1) Long blind range regions due to eclipsing during transmission (2) Reduced Doppler tolerance of the individual pulse. A matched filter designed for non-zero Doppler is usually created using inter-pulse compensation of the Doppler-induced phase-ramp (usually through fast Fourier transform - FFT). On the other hand intra-pulse phase-ramp compensation is rarely implemented. Therefore, the longer the pulse the larger is the destructive phase difference accumulated during its duration by the uncompensated Doppler-induced phase-ramp.

The other way to raise the energy - increasing the number of pulses within a given CPI - implies a radar mode of medium or high pulse repetition frequency (PRF). These modes can suffer from range ambiguity because the delay of returns from distant targets can be longer than the pulse repetition interval (PRI). The common approach to resolve range ambiguity is to use several CPIs within a single dwell; each CPI with a different PRF. Resolving the true range and Doppler is performed non-coherently, using an "H out of P" decision, where H is usually 2 or 3 PRFs, while P can be as large as 8 PRFs [2, 3]. A "2 out of 8" detection decision implies that in some cases only 2 out of the 8 CPIs contribute energy to the detection process. This is a rather inefficient use of the transmitted energy.

This paper suggests an alternative approach to mitigate the range ambiguity in high PRF. It employs inter-pulse coding during a single CPI that may occupy the entire dwell. A convenient coding is based on an Ipatov binary sequence [4, 5], which yields ideal, low-loss, periodic cross-correlation with a slightly mismatched sequence. In order to exploit the sidelobe-free periodic cross-correlation, the number N_s of consecutive transmitted sequences has to be larger than the number N_r of reference sequences stored in the receiver, by at least two, (e.g., N_s =18 and N_r = 16). Ternary or polyphase codes, with ideal periodic correlation, can also be used.

The suggested concept applies to low peak-power radar (electromagnetic or acoustic) that has to cover both close and mid range. The low peak-power restriction implies that the radar receiver is not blanked nor is it saturated during direct reception of the transmission, and the receiver can always perform linear processing.

2. COMPARING INTRA-PULSE AND INTER-PULSE CODING

The comparison will be between a high-PRF pulse train with inter-pulse coding based on Ipatov 13 code (Fig. 1), and a low-PRF pulse-train with intra-pulse Barker 13 coding, (Fig. 2). The two signals have identical energy, peak power, CPI duration and range resolution. The reflected Ipatov signal is correlated with a slightly mismatched reference sequence. The signal and the reference are listed in Table 1. The horizontal time axis is in units of the pulse repetition period T_r.

1-4244-1539-X/08/$25.00 ©2008 IEEE

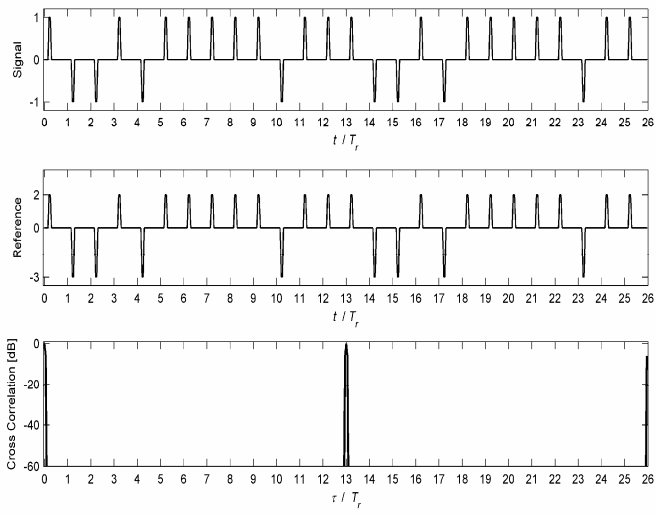

Figure 1 – Two periods out of a high PRF pulse train with inter-pulse coding based on Ipatov 13 sequence: Signal (top), reference (middle), periodic cross-correlation (bottom).

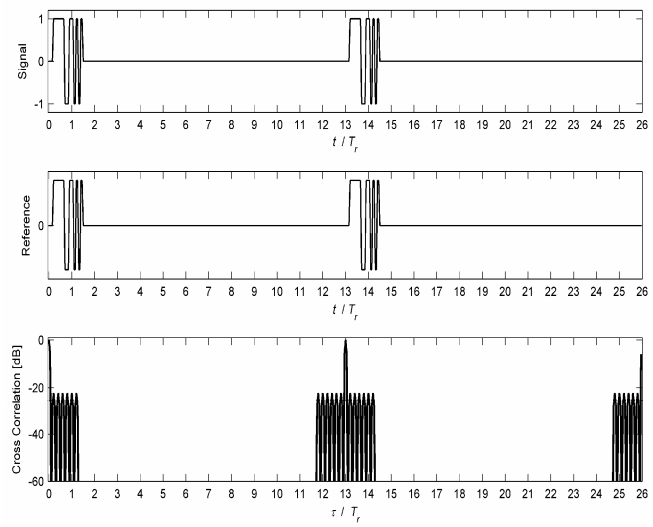

Figure 2 – Two periods out of a low PRF pulse train with intra-pulse coding based on Barker 13 sequence: Signal (top), matched reference (middle), periodic cross-correlation (bottom).

Sig	1	–1	–1	1	–1	1	1	1	1	1	–1	1	1
Ref	2	–3	–3	2	–3	2	2	2	2	2	–3	2	2

Table 1 – Ipatov 13 code and reference

Note the sidelobe-free correlation output in the lower subplot of Fig. 1, with a periodicity of $13T_r$. The PRI of the Barker-coded signal was set at the same $13T_r$ to get the same periodicity. The pulse duration here is 13 time longer. The response of a matched filter (Fig. 2, bottom subplot) exhibits sidelobes (-22 dB), extending, in each side, for the pulse duration. If a mismatched filter is used, the sidelobes can be made lower but wider, with small SNR loss.

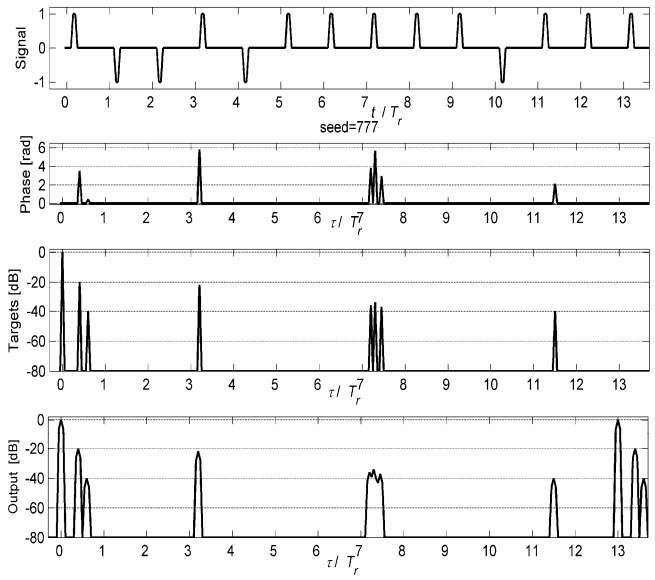

Figure 3 – Detecting a target scene using inter-pulse coding.

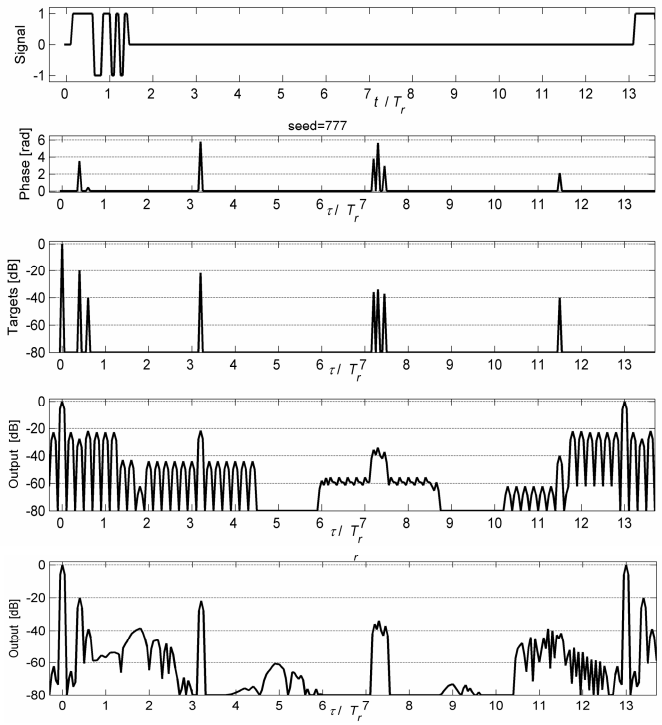

Figure 4 – Detecting a target scene using intra-pulse coding.

The results achieved by the two signals, in the presence of targets, are demonstrated in Figs. 3 and 4, obtained from numerical simulations. The time axis in all the subplots in the two figures are equal and extends over 13 basic repetition periods T_r. Consider first Fig. 3, which applies to the inter-pulse coded signal. The top subplot shows one period (out of 8) of the transmitted Ipatov 13 pulse sequence. The width of each pulse is $t_b = 0.1T_r$. The beginning of the next sequence is also seen starting at $t = 13\,T_r$. The targets are de-

scribed in the 2nd and 3rd subplots. Targets were placed only within the delay span $0 \le \tau \le 13\,T_r$. The "target" at zero delay represents the reception of the transmitted signal, and will be referred to as the "direct signal". Each target is described by its phase in radians (2nd subplot) and its magnitude in dB (3rd subplot). Note that this was a noise-free simulation and the targets were stationary. The 4th subplot displays the output (magnitude) of the correlation with the reference pulse sequence (see Table 1). Comparing the two bottom subplots shows that the output replicates the targets very well, without adding any sidelobes. Of course, the targets picture repeats itself after $\tau = 13\,T_r$, as expected in both signals.

We now turn to Fig. 4, which applies to the intra-pulse coded signal. The top subplot shows one period (out of 8) of the transmitted Barker 13 signal. The pulse duration is $t_p = 13\,t_b = 1.3T_r$. The beginning of the next pulse is also seen, starting at $t = 13\,T_r$. The targets are described in the 2nd and 3rd subplots. The 4th subplot displays the output (magnitude) of the matched filter. The last (bottom) subplot displays the output of a mismatched filter of length 39 designed for minimum integrated sidelobes. Comparing the two lower subplots with the targets subplot we note that in the matched-filter case the sidelobes of the direct signal mask the first two targets. The last target is also barely distinguishable from the sidelobes of the folded direct signal (centred at $\tau = 13\,T_r$). Using a mismatched filter reduced the masking effect, but created more distant sidelobes that can be mistaken as targets. In general, the presence of sidelobes is quite dominant, and if more weak targets were present, many would have been obscured by sidelobes.

3. RESULTS FROM ACOUSTIC SIMULATOR

The two signals described above were implemented in J. Mike Baden's indoor acoustic radar. The unambiguous range was 2.6 meters. A corner reflector was placed about 0.4 meters before the ambiguous range. The processed reflected scene is plotted in Fig. 5. The intra-pulse coded Barker 13 signal was processed on-receive by both a matched-filter (length 13) and a mismatched filter (length 78). The corresponding outputs are shown in the top and middle subplots, respectively. The relatively high (-22dB) sidelobes of the Barker 13 matched response are very prominent in the top subplot, especially around the direct signal, the ambiguous range and the corner reflector.

The inter-pulse coded Ipatov 13 signal was processed using its nominal mismatched filter given in Table 1. Its processor output is shown in the bottom subplot of Fig. 5. In principle this output should be sidelobes-free and we should deduce that the bottom subplot contains only genuine target and clutter returns. (The noise level is well below -80 dB.) The middle subplot can serve as a judge. The middle subplot was obtained from the Barker 13 signal using a 78 element mismatched filter designed for minimum integrated sidelobes (ISL). Its peak sidelobe (PSL) is -65dB. Hence the mid subplot can be assumed as almost sidelobe-free. Indeed the middle subplot strongly resembles the bottom subplot, thus supporting the theoretical conclusion that the inter-pulse periodic Ipatov coding yields sidelobe-free response.

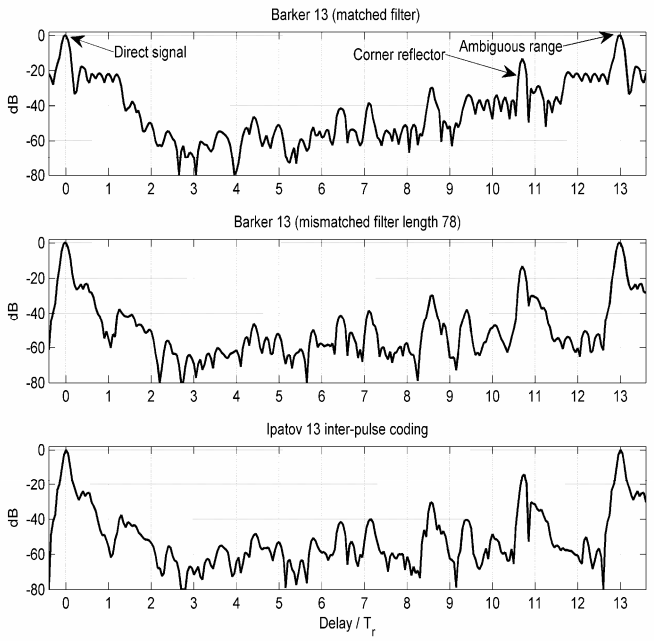

Fig. 5 - Results from indoor acoustic simulator

4. DELAY-DOPPLER RESPONSE

A longer sequence - Ipatov 24 - will be used to demonstrate the delay-Doppler response when the receiver performs coherent cross-correlation with the nominal mismatched filter. The binary coding of the transmitted pulse sequence is given in the top row of Table 2 and its nominal reference in the bottom row. Note that in the Ipatov 24 case, the reference is a three-valued sequence. When calculating the delay-Doppler response we used N_s =18 periods of the transmitted signal and N_r = 16 periods of the reference (each period contains M = 24 pulses). Hence, the total number of pulses processed coherently was $N_r M$ (= 384). The overall duration of the CPI was therefore $N_r M\ T_r$.

Fig. 6 displays the magnitude of the delay-Doppler periodic response $|\psi(\tau,\nu)|$ for the delay span $|\tau| < 1.1T_r$ and Doppler span of $0 \le \nu \le 1.2/MT_r$. We can refer to $\psi(\tau,\nu)$ as *periodic* because $N_r + 2 \le N_s$.

Sig	+1	+1	+1	−1	−1	−1	+1	−1	−1	−1	−1	−1	+1	−1	−1	+1	−1	+1	+1	−1	−1	−1	+1	−1
Ref	+5	+11	+11	−7	−7	−7	+5	−7	−7	−7	−7	−7	+5	−7	−7	+11	−7	+11	+5	−7	−7	−7	+11	−7

Table 2 - Ipatov 24 sequence

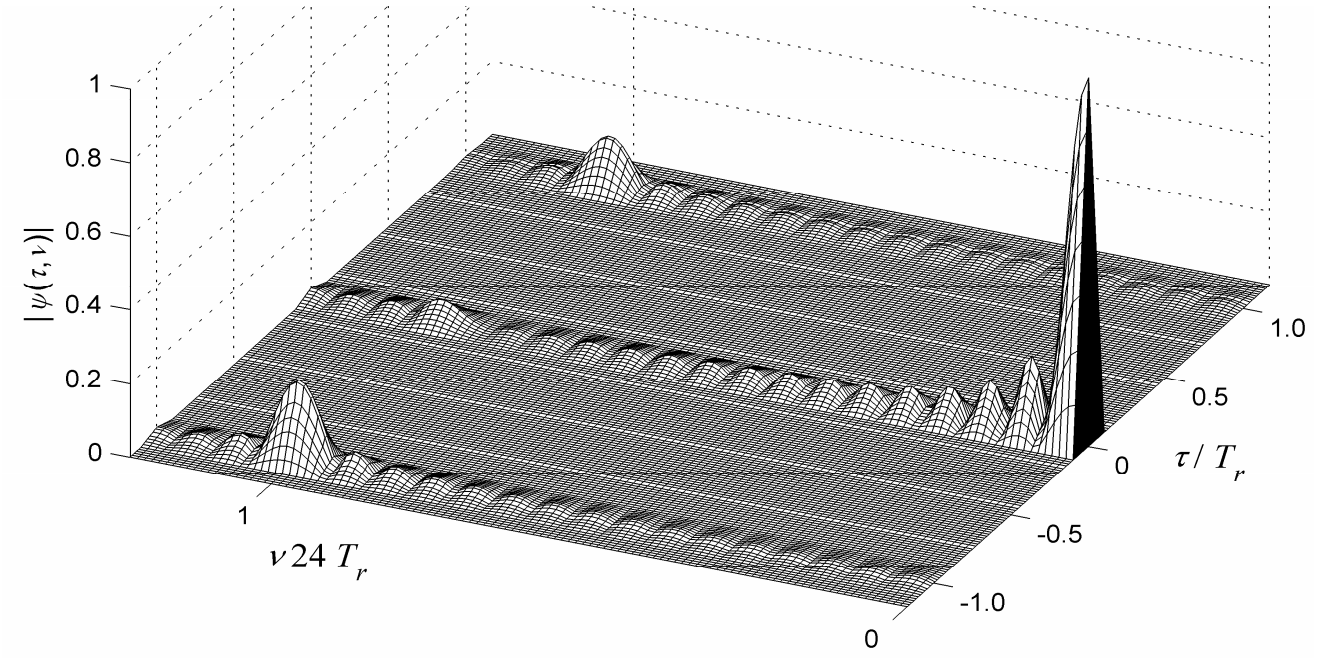

Figure 6 - Delay-Doppler periodic response of 16 periods of a signal based on an Ipatov 24 sequence. Zoom on $|\tau| < 1.1T_r$ and $0 \le \nu \le 1.2/MT_r$.

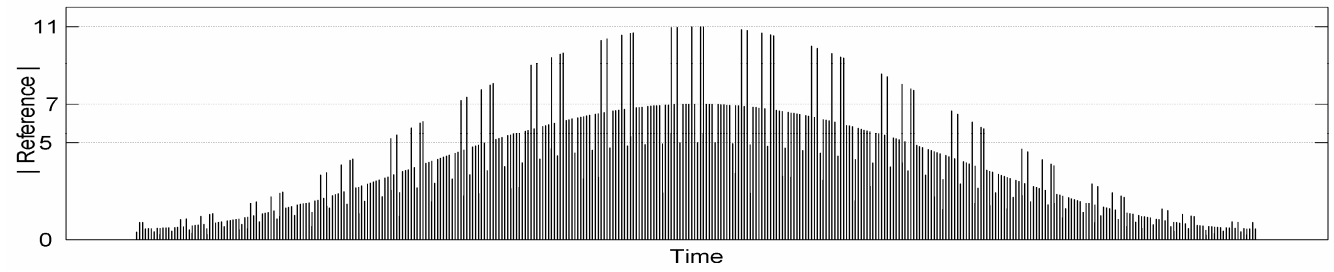

Figure 7 - Hamming-weighted amplitude of 16 periods of the reference pulse train (based on Ipatov 24 sequence)

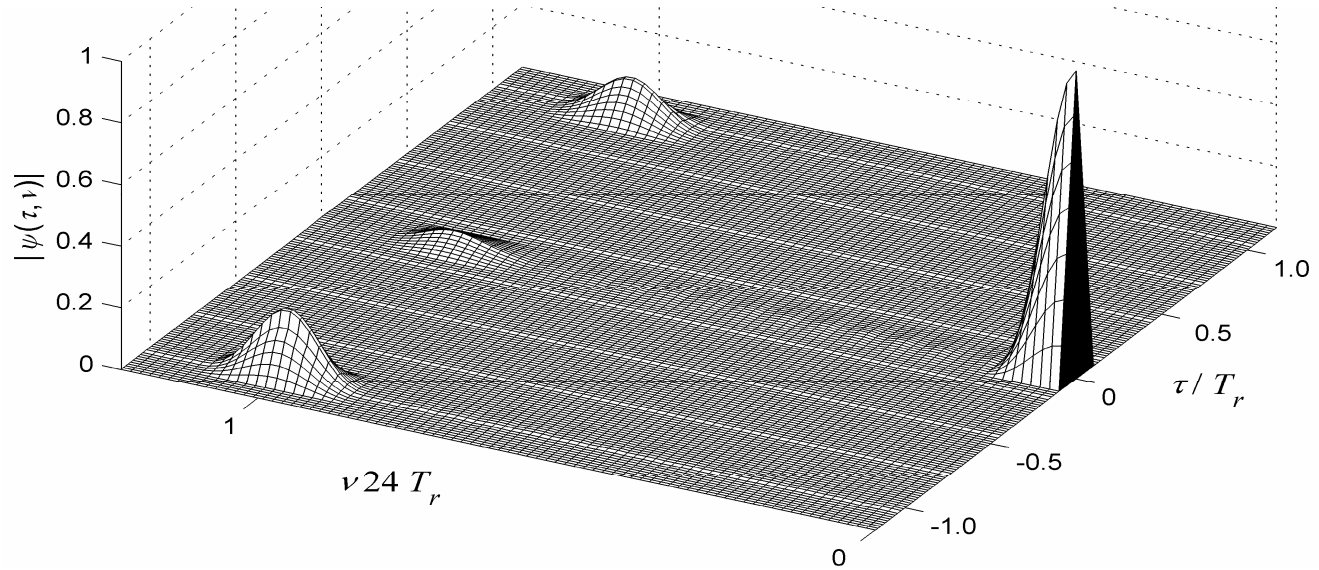

Figure 8 - Delay-Doppler periodic response of 16 periods of a signal based on an Ipatov 24 sequence, with Hamming-weighted reference. Zoom on $|\tau| < 1.1T_r$ and $0 \le \nu \le 1.2/MT_r$.

The most important result is the fact that the property of no recurrent lobes at $\tau = \pm T_r, \nu = 0$ extends to higher Doppler values. However, at $\tau = \pm T_r$ we see slow build-up of sidelobes with Doppler, becoming small peaks at the inverse of the sequence period, namely at $\nu = 1/MT_r = 1/24\,T_r$. The mainlobe extends in delay over $|\tau| < t_p$, and in Doppler it reaches its first null at the inverse of the CPI duration, namely at $\nu = 1/N_r MT_r = 1/384\,T_r$ (not marked). The Doppler sidelobes behavior follows a sinc function.

The Doppler sidelobes can be lowered by amplitude weighting the reference signal. The amplitudes of a Hamming-weighted reference pulse train (384 pulses) are shown in Fig. 7. Fig. 8 displays the delay-Doppler response when the unweighted signal is cross-correlated with the Hamming-weighted reference. Fig. 8 covers the same delay-Doppler span as Fig. 6. Comparing the two figures shows lower Doppler sidelobes but an increase in the Doppler width of the mainlobe and of the recurrent Doppler lobes at $\nu = 1/MT_r = 1/24\,T_r$. Adding Hamming weight only in the receiver adds SNR loss of about 1.5 dB.

A broader picture of the delay-Doppler response, when the reference is Hamming-weighted, is shown in Fig. 9.

Here the delay axis extends slightly beyond the delay recurrent lobes, at $\tau = \pm MT_r = \pm 24\,T_r$. Because the transmitted signal is longer than the reference signal by at least two sequence periods, the first recurrent lobes (one on each side) are identical to the mainlobe. Without coding there should have been recurrent delay lobes at $\tau = \pm nT_r$, $n = 1, 2, \ldots$. Fig. 9 demonstrates the absence of recurrent delay lobes (at zero Doppler) up to and including $n = M - 1 = 23$. Lower recurrent lobes of varying peaks do appear at high Doppler around $\nu = 1/MT_r = 1/24\,T_r$.

A "bed of nails" response, with recurrent main lobes in both delay and Doppler, but free from delay sidelobes, can also be obtained from inter-pulse coding. This requires coding by a chirp-like poly-phase sequence. An example of an even length phase sequence is: $\phi_m = \pi m^2/M,\ m = 0, 1, \ldots, M-1$. Fig. 10 displays the resulted delay-Doppler response (M=24).

For comparison, Fig. 11 shows the delay-Doppler response of a conventional coherent train of 16 pulses, intra-pulse coded by a 24 element MPSL code (see Table 6.3 in [5]), with Hamming weight on receive. The PRI is 24 times that of the previous signal, in order to get the same range ambiguity and CPI duration. This "bed of nails" response exhibits delay sidelobes extending on both sides of each main lobe, for the pulse duration $(\pm 24\,t_b)$.

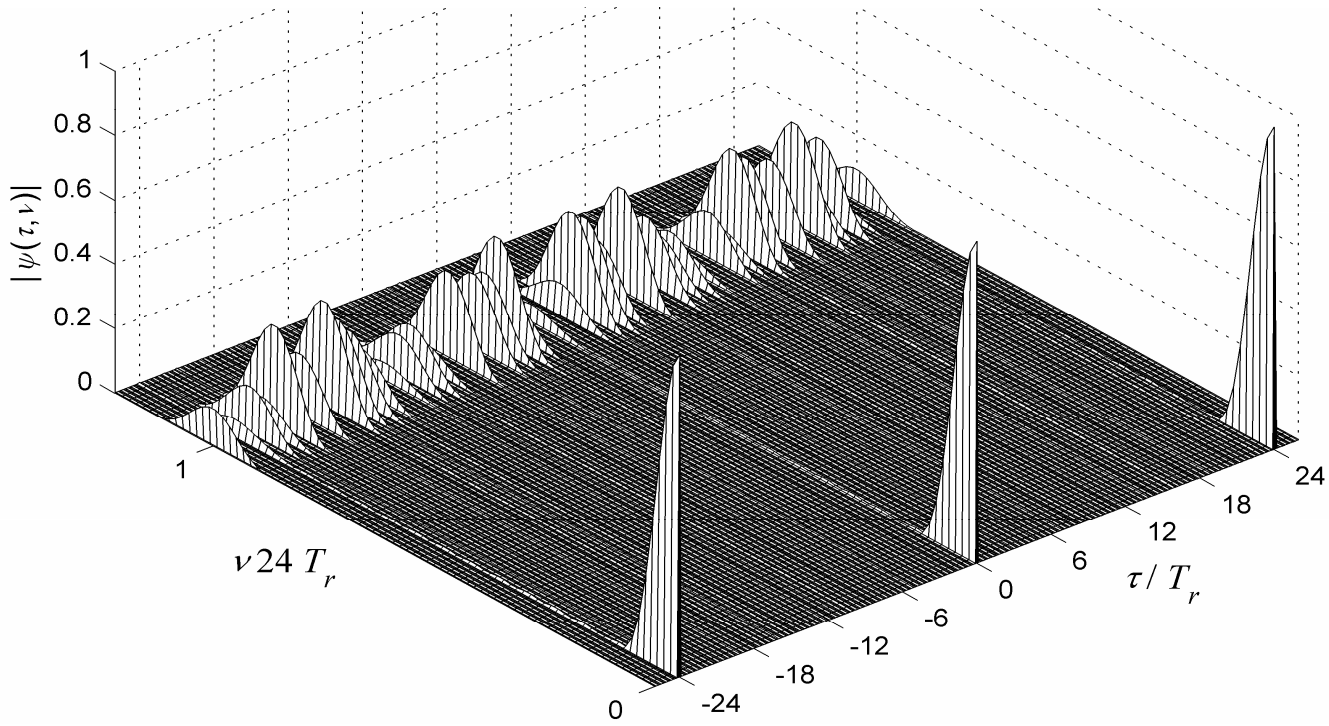

Figure 9 - Delay-Doppler periodic response of 16 pulse train sequences, each inter-pulse coded by an Ipatov 24 binary sequence, with Hamming-weighted reference. Zoom on $|\tau| < (M+1)T_r$ and $0 \le \nu \le 1.2/MT_r$.

5. CONCLUSIONS

We showed how to transfer the task of pulse compression from a single long coded pulse to many short pulses with inter-pulse coding. The described inter-pulse coding was based on sequences with ideal periodic correlation. For simple binary transmission we recommended Ipatov binary sequences, which exhibit ideal (sidelobe-free) cross-correlation with a slightly mismatched reference sequence. Ipatov's ternary sequences [6] could also be used. In a ternary sequence a "0" element implies skipping a pulse. Another possibility is any one of the many poly-phase sequences with ideal periodic correlation. To maintain the periodic property the number of transmitted sequences has to exceed the number of reference sequences by at least two. Using this kind of coding, the effective periodicity increases from the actual pulse repetition period to the much longer sequence repetition period; thus mitigating range ambiguity and target folding. Combining intra and inter-pulse coding is possible. Since the correlation receiver needs to perform linear processing, the transmitter/receiver isolation must be large enough so that the direct signal will not cause saturation or blanking of the receiver.

REFERENCES

[1] W. H. Long and K. A. Harriger, "Medium PRF for the AN/APG-66 radar," *Proceedings of the IEEE*, vol. 73, pp. 301-311, Feb. 1985.

[2] S. A. Hovanessian, "An algorithm for calculation of range in multiple PRF radar," *IEEE Transactions on Aerospace and Electronic Systems*,, vol. AES-12, pp. 287-290, Mar. 1976.

[3] D. Wiley, S. Parry, C. Alabaster, and E. Hughes, "Performance comparison of PRF schedules for medium PRF radar," *IEEE Transactions on Aerospace and Electronic Systems*, vol. 42, pp. 601-611, Apr. 2006.

[4] V. P. Ipatov, and B. V. Fedorov, "Regular binary sequences with small losses in suppressing sidelobes," *Radioelectronic and Communication Sysems, (Radioelektronica)*, vol. 27, 3, pp. 29-33, 1984.

[5] N. Levanon and E. Mozeson, *Radar Signals*. Hoboken, NJ: Wiley, 2004, Sec. 6.5.

[6] V. P. Ipatov, "Ternary sequences with ideal periodic autocorrelation," *Radio Engineering and Electronic Physics*, vol. 24, 10, pp. 75-79, 1979.

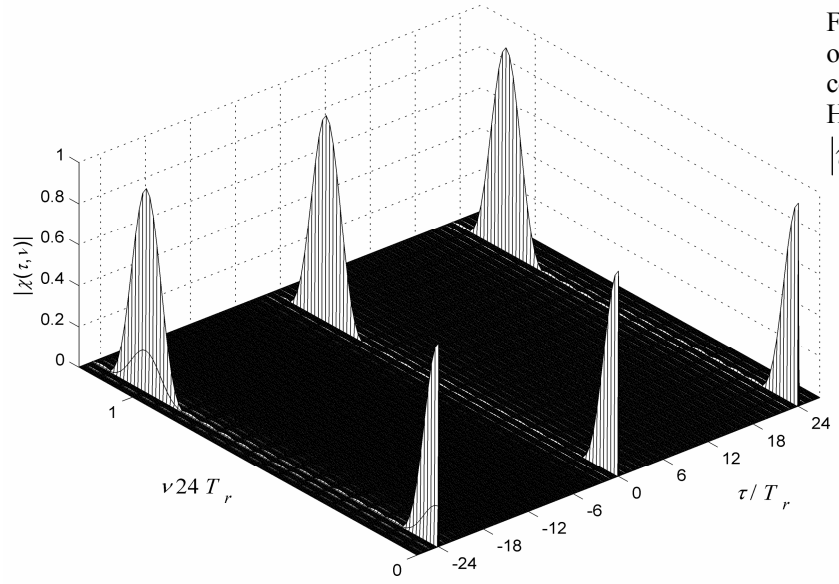

Figure 10 - Delay-Doppler periodic response of 16 pulse train sequences, each inter-pulse coded by a 24 element poly-phase code, with Hamming-weighted reference. Zoom on $|\tau| < (M+1)T_r$ and $0 \le \nu \le 1.2/MT_r$.

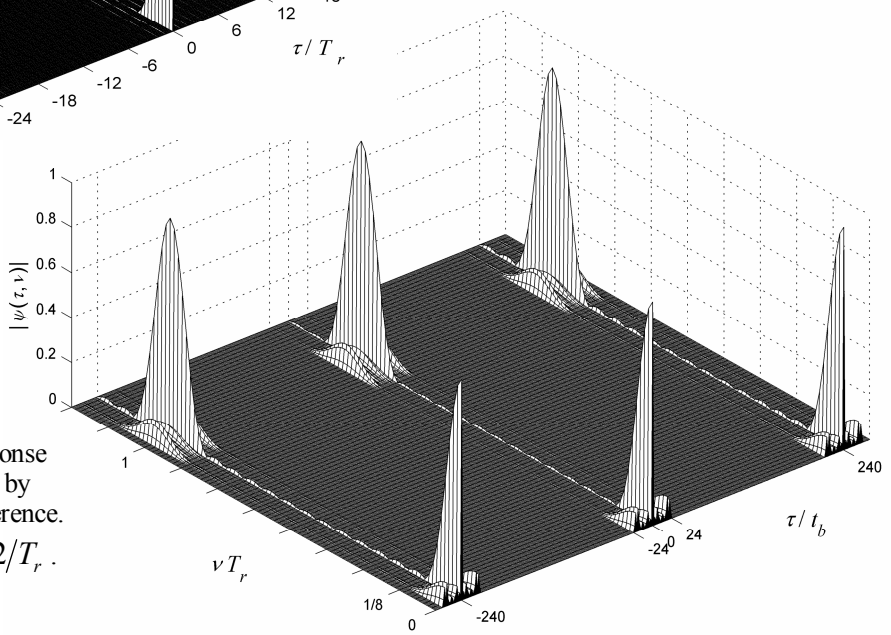

Figure 11 - Delay-Doppler periodic response of a train of 16 pulses, intra-pulse coded by MPSL 24, with Hamming-weighted reference. Zoom on $|\tau| < 1.2T_r$ and $0 \le \nu \le 1.2/T_r$.